

# The first known Uranian Trojan and the frequency of temporary giant-planet co-orbitals.

Mike Alexandersen,<sup>1\*</sup> Brett Gladman,<sup>1</sup> Sarah Greenstreet,<sup>1</sup>  
J.J. Kavelaars,<sup>2</sup> Jean-Marc Petit<sup>3</sup>

<sup>1</sup>Department of Physics and Astronomy, University of British Columbia,  
6224 Agricultural Road, Vancouver, BC V6T 1Z1, Canada

<sup>2</sup>National Research Council of Canada, Victoria, BC V9E 2E7, Canada

<sup>3</sup>Institut UTINAM, CNRS-UMR 6213, Observatoire de Besançon,  
BP 1615, 25010 Besançon Cedex, France

\*E-mail: mikea@astro.ubc.ca

Trojan objects share a planet's orbit, never straying far from the triangular Lagrangian points,  $60^\circ$  ahead of or behind the planet. We report the first discovery of a Uranian Trojan: 2011 QF<sub>99</sub> oscillates around the Uranian L4 Lagrange point for  $> 70$  kyr and remains co-orbital (in 1:1 resonance) for  $\sim 1$  Myr before becoming a Centaur. Instead of being a primordial Trojan, it must be a temporary co-orbital. We construct a steady-state Centaur model, supplied from the transneptunian region, to investigate the frequency and duration of temporary co-orbital captures, finding that at any time large fractions (0.5% and 1.9%) of the population will be Uranian and Neptunian co-orbitals, respectively. We show for the first time that the high co-orbital Centaur fraction ( $\sim 3\%$ ) in the IAU Minor Planet Centre database is that expected under transneptunian steady-state supply.

During 2011 and 2012, we used the Canada-France-Hawaii Telescope (CFHT) to performed a 20 square degree survey designed to discover of order 100 Trans-Neptunian Objects (TNOs) and Centaurs with  $m_r < 24.5$  and then track all detections for up to 17 months. The project was accurately calibrated in order to constrain the size and orbital parameter distributions of populations resonant with Neptune, for which the observations were optimised (see appendix).

One discovery was of particular interest, designated 2011 QF<sub>99</sub> (Alexandersen et al., 2013). 2011 QF<sub>99</sub> was discovered at a heliocentric distance of 20.3 AU, where its apparent magnitude  $m_r = 22.6 \pm 0.1$  sets its absolute magnitude at  $H_r = 9.6$  ( $H_g = 10.3$  for a typical colour  $g - r \approx 0.7$ ). This magnitude indicates that 2011 QF<sub>99</sub> is  $\sim 60$  km in diameter, assuming a 5% albedo. As more observations constrained the orbit, it became clear that 2011 QF<sub>99</sub> was not simply a Centaur that happened to be near the distance of Uranus. Our current astrometry, including 29 astrometric measurements of 2011 QF<sub>99</sub> from 7 dark-runs with a total arc of 419 days, indicates the following orbital elements:  $a = 19.090 \pm 0.004$  AU,  $e = 0.1765 \pm 0.0007$ ,  $i = 10^\circ 8' 11'' \pm 0^\circ 0' 01''$ ,  $\Omega = 222^\circ 49' 8'' \pm 0^\circ 0' 01''$ ,  $\omega = 287^\circ 51' \pm 0^\circ 11'$ ,  $T = 246\,4388 \pm 11$  JD. Here  $a$ ,  $e$ ,  $i$ ,  $\Omega$ ,  $\omega$ ,  $T$  are the osculating J2000 barycentric semi-major axis, eccentricity, inclination, longitude of ascending node, argument of pericentre and Julian day of pericentre. The low eccentricity along with a semi-major axis similar to that of Uranus ( $a_U \approx 19.2$  AU) indicated that 2011 QF<sub>99</sub> could potentially be a Uranian co-orbital. Co-orbital bodies are in the 1:1 mean-motion resonance with a planet (thus having the same orbital period) and a librating (oscillating) resonant angle  $\phi_{11} = \lambda - \lambda_{Planet}$ . Here  $\lambda$  is the mean longitude, which is the sum of  $\Omega$ ,  $\omega$  and the mean anomaly.  $\phi_{11}$  roughly measures how far ahead in orbital phase the object is relative to the planet. For co-orbital motion,  $\phi_{11}$  librates around one of four values (Mikkola et al., 2006). Quasi-satellites librate around  $0^\circ$ ; in the co-orbital reference frame these appear to move like retrograde satellites, despite being outside the planet's domain of gravitational dominance. Leading and trailing Trojans librate around L4 ( $60^\circ$  ahead of planet) and L5

( $300^\circ$  ahead =  $60^\circ$  behind planet), respectively. Horseshoe orbits librate around  $180^\circ$  with high amplitude librations that encompasses all of the L3, L4 and L5 Lagrange points.

A short numerical integration (50 kyr) showed that 2011 QF<sub>99</sub> is indeed librating around the leading (L4) Lagrange point (see Fig. 1). Could 2011 QF<sub>99</sub> be a primordial Trojan? Jupiter has long been known to host a large population of Trojan asteroids which are stable on time scales of several Gyr. The more recently discovered stable population of Neptunian Trojans are now believed to outnumber the Jovian Trojans for objects with radius larger than 50 km (Chiang and Lithwick, 2005; Sheppard and Trujillo, 2010b). In contrast, the Trojan regions of Saturn and Uranus are believed to be mostly unstable (Nesvorný and Dones, 2002; Dvorak et al., 2010) and are unlikely to host long-lived Trojans, although a few stable niches may exist if one ignores the instability generated during giant planet migration (Dvorak et al., 2010).

In longer integrations, using the 10 Myr time scale typically used to determine the dynamical class of outer Solar System objects (Gladman et al., 2008; Lykawka and Mukai, 2007), we find that both the nominal orbit of 2011 QF<sub>99</sub> and all other orbits within the (already small) orbital uncertainties librate around the L4 Lagrange point for at least the next 70 kyr (Fig. 2 left column, and Fig. A1). On time scales of 100 kyr to 1 Myr, all integrated orbits transition out of the L4 Trojan region (see appendix), either escaping directly to scattering behaviour (that is, become Centaurs) or transitioning to other co-orbital behaviour before ceasing co-orbital behaviour and scattering away within 3 Myr. We considered the remote possibility that a small niche in phase space, stable for 4 Gyr, could exist within the uncertainty range without being found by the initial investigation, or that systematic errors could result in the real orbit being offset by many times the nominal uncertainties. We thus integrated 6000 test particles filling the region within  $\Delta a \pm 0.4$  AU,  $\Delta e \pm 0.03$ , and  $\Delta i \pm 2^\circ$  of the nominal orbit for 1 Gyr. All but 33 of these particles were ejected from the Solar System in the 1 Gyr integration, most within the usual 10 Myr stability of Centaurs (Dones et al., 1999; Tiscareno and Malhotra, 2003), and all survivors

were out in the  $a > 30$  AU scattering disk. We thus feel there is no chance that 2011 QF<sub>99</sub> has been a Uranian Trojan for very long, and must instead be a Centaur recently trapped temporarily into L4 libration.

Temporary co-orbitals are known elsewhere in the Solar System (see appendix for details). In our current survey, 2011 QF<sub>99</sub> was the only object with a semi-major axis within the planetary region (defined here as  $a < 34$  AU to include Neptune co-orbitals but exclude the exterior stable transneptunian populations). The Canada-France Ecliptic Plane Survey (CFEPS) discovered three  $a < 34$  AU objects and the IAU Minor Planet Centre (MPC) database contains 173 objects with  $6 \text{ AU} < a < 34 \text{ AU}$  as of 2013-Jan-01. We seek to determine if (at least to order of magnitude) it is reasonable that, in a steady-state model of Centaur supply from the scattering disk, enough objects should be in resonance at any time to explain the observed discovery of 2011 QF<sub>99</sub> and other temporary co-orbitals. In other words, is co-orbital trapping sufficiently frequent and long-lived that one should expect to observe these temporary objects or is another source required? To address this, we estimated the steady-state fraction of Centaurs in temporary co-orbital states with Uranus and Neptune, similar to what has been done for the Earth (Morais and Morbidelli, 2002) and Venus (Morais and Morbidelli, 2006).

Using a model of the orbital distribution (Kaib et al., 2011) giving today's scattering (Gladman et al., 2008) TNOs (see appendix), we simulated the interactions of TNOs and Centaurs with the giant planets over 1 Gyr, building a steady-state distribution for the  $a < 34$  AU region. Particles were removed from the simulation if they hit a planet, went outside 2000 AU or inside 6 AU from the Sun (as the latter mostly are rapidly removed from the Solar System by Jupiter). The simulation outputs the location of the planets and all  $a < 34$  AU particles at 300 yr intervals. The output interval was chosen so that the few-kyr variation of the resonant argument  $\phi_{11}$  would be well sampled; to our knowledge, this is the first time such a meticulous search for short-term co-orbitals has been performed for an armada of incoming scattering objects. An earlier analysis (Horner and Wyn Evans, 2006)

of the giant planets temporarily capturing Centaurs started with some currently known Centaurs, which is biased towards the lowest- $a$  Centaurs due to observational selection, resulting in much lower capture rates for Uranus and Neptune than we find. Fig. 2 shows two examples from our simulations of Centaurs trapped in Trojan orbits over similar time scales as 2011 QF<sub>99</sub>.

The simulations show that scattering objects predominantly enter the giant planet region ( $a < 34$  AU) at intermediate inclinations and eccentricities, as has been previously shown (Levison and Duncan, 1997; Tiscareno and Malhotra, 2003). After analysing the particle histories to find co-orbital trapping (see appendix), we find that 0.5% and 1.9% of the steady-state  $a < 34$  AU population is, at any time, in co-orbital motion with Uranus and Neptune, respectively. This surprisingly large fraction,  $\approx 2.5\%$ , dwarfs the  $\approx 0.1\%$  of near Earth asteroids temporarily trapped in Earth and Venus co-orbital motion (Morais and Morbidelli, 2002, 2006), presumably due to the fractionally larger giant planet cross-section and lower encounter speeds. For the Neptunian co-orbitals, 36% of their time was spent in horseshoe orbits, 13% as quasi-satellites (see appendix) and 51% as Trojans, equally distributed between the leading and trailing clouds. The Uranians, typically captured from higher relative velocities, had more horseshoes (74%), with only 7% quasi-satellites and 19% Trojans. The duration of Uranian co-orbital captures in our simulation had mean, median and maximum values of 114 kyr, 59 kyr and 2.7 Myr, respectively. For Neptunian captures, these values were 84 kyr, 45 kyr and 18.2 Myr, respectively.

To explore the strength of observational biases, we use the CFEPS Survey Simulator (Gladman et al., 2012), expanded to include our new coverage. The survey simulator applies observational biases to the model intrinsic population from the dynamical simulation (see appendix) in order to simulate what a survey would in fact observe. The absolute  $H$ -magnitude distribution (a proxy for the size distribution) of the objects is very important when modelling flux limited surveys. A first attempt to use a single exponential distribution ( $dN/dH \propto 10^{\alpha H}$ , see appendix) with  $\alpha \approx 0.8$ , as measured for  $H_g < 9.0$  TNOs (Elliot

et al., 2005; Petit et al., 2011) and Neptunian Trojans (Sheppard and Trujillo, 2010b) was highly rejectable, predicting that small ( $H_g > 11.0$ ) objects should accounting for 81% of the detections; our observations have no such objects. Previous work (Sheppard and Trujillo, 2010b) has established that the  $H$ -mag distribution of Neptunian Trojans cannot continue as a single exponential beyond  $m_R \approx 23.5$  ( $H_g \approx 9.3$  using  $g - R = 0.5$  and a typical distance of 30 AU). Recent work (Shankman et al., 2013) found that the scattering objects reject a single exponential and are better represented by a “divot”  $H$ -mag distribution, where the number density drops at  $H_g \approx 9.0$  by a contrast factor (the ratio of number density just before the divot to just after) of 6 and then continues with a second shallower exponential with  $\alpha \approx 0.5$ . Although we lack the statistics to independently constrain a divot  $H$ -mag distribution, when simply adopting the above parameters we find a much better agreement between the simulated and observed populations (see Fig. 3), with the small ( $H_g > 11.0$ ) objects now only providing 23% of the detections.

Simulating our current calibrated fields, we find that of the  $a < 34$  AU detections, 1.1% should be Uranian co-orbitals and 1.8% should be Neptunian co-orbitals (Fig. 3). Comparing to the intrinsic fractions, one sees that, due to where we looked and the survey limits, detection of Uranian co-orbitals was enhanced compared to the intrinsic fraction (0.5%), while the Neptunian co-orbitals did not experience a significant bias. Of the 173 objects with  $6 \text{ AU} < a < 34 \text{ AU}$  currently in the MPC database, around six (including 2011 QF<sub>99</sub>) have been identified as temporary co-orbitals of Uranus and Neptune (see appendix), yielding  $\sim 3\%$ . This is close to our model prediction of 3%, although the unknown pointing history and survey depths make detailed modelling impossible. However, our simulations show that no large biases exist towards or against detecting co-orbitals, suggesting that the MPC co-orbital fraction may be close (within a factor of a few) to the intrinsic fraction. We thus believe that this first detected Uranian Trojan, 2011 QF<sub>99</sub>, is part of a steady-state population of transient co-orbitals, temporarily (although sometimes for millions of years) trapped by the giant planets.

## References

- Alexandersen, M., Kavelaars, J., Petit, J., Gladman, B., and Williams, G. V. (2013). 2011 QF99. *Minor Planet Electronic Circulars*, page 19.
- Bottke, W. F., Jedicke, R., Morbidelli, A., Petit, J.-M., and Gladman, B. (2000). Understanding the Distribution of Near-Earth Asteroids. *Science*, 288:2190–2194.
- Brasser, R., Mikkola, S., Huang, T.-Y., Wiegert, P., and Innanen, K. (2004). Long-term evolution of the Neptune Trojan 2001 QR322. *Monthly Notices of the Royal Astronomical Society*, 347:833–836.
- Chiang, E. I., Jordan, A. B., Millis, R. L., Buie, M. W., Wasserman, L. H., Elliot, J. L., Kern, S. D., Trilling, D. E., Meech, K. J., and Wagner, R. M. (2003). Resonance Occupation in the Kuiper Belt: Case Examples of the 5:2 and Trojan Resonances. *Astronomical Journal*, 126:430–443, arXiv:astro-ph/0301458.
- Chiang, E. I. and Lithwick, Y. (2005). Neptune Trojans as a Test Bed for Planet Formation. *Astrophysical Journal*, 628:520–532, arXiv:astro-ph/0502276.
- Connors, M., Chodas, P., Mikkola, S., Wiegert, P., Veillet, C., and Innanen, K. (2002). Discovery of an asteroid and quasi-satellite in an Earth-like horseshoe orbit. *Meteoritics and Planetary Science*, 37:1435–1441.
- Connors, M., Veillet, C., Brasser, R., Wiegert, P., Chodas, P., Mikkola, S., and Innanen, K. (2004). Discovery of Earth’s quasi-satellite. *Meteoritics and Planetary Science*, 39:1251–1255.
- de la Fuente Marcos, C. and de la Fuente Marcos, R. (2012a). (309239) 2007 RW<sub>10</sub>: a large temporary quasi-satellite of Neptune. *Astronomy and Astrophysics*, 545:L9, 1209.1577.

- de la Fuente Marcos, C. and de la Fuente Marcos, R. (2012b). Four temporary Neptune co-orbitals: (148975) 2001 XA<sub>255</sub>, (310071) 2010 KR<sub>59</sub>, (316179) 2010 EN<sub>65</sub>, and 2012 GX<sub>17</sub>. *Astronomy and Astrophysics*, 547:L2, 1210.3466.
- de la Fuente Marcos, C. and de la Fuente Marcos, R. (2013). Crantor, a short-lived horseshoe companion to Uranus. *ArXiv e-prints*, 1301.0770.
- Dones, L., Gladman, B., Melosh, H. J., Tonks, W. B., Levison, H. F., and Duncan, M. (1999). Dynamical Lifetimes and Final Fates of Small Bodies: Orbit Integrations vs Öpik Calculations. *Icarus*, 142:509–524.
- Dvorak, R., Bazzó, Á., and Zhou, L.-Y. (2010). Where are the Uranus Trojans? *Celestial Mechanics and Dynamical Astronomy*, 107:51–62, 0911.2366.
- Elliot, J. L., Kern, S. D., Clancy, K. B., Gulbis, A. A. S., Millis, R. L., Buie, M. W., Wasserman, L. H., Chiang, E. I., Jordan, A. B., Trilling, D. E., and Meech, K. J. (2005). The Deep Ecliptic Survey: A Search for Kuiper Belt Objects and Centaurs. II. Dynamical Classification, the Kuiper Belt Plane, and the Core Population. *Astronomical Journal*, 129:1117–1162.
- Gladman, B., Lawler, S. M., Petit, J.-M., Kavelaars, J., Jones, R. L., Parker, J. W., Van Laerhoven, C., Nicholson, P., Rousselot, P., Bieryla, A., and Ashby, M. L. N. (2012). The Resonant Trans-Neptunian Populations. *Astronomical Journal*, 144:23, 1205.7065.
- Gladman, B., Marsden, B. G., and Vanlaerhoven, C. (2008). *Nomenclature in the Outer Solar System*, pages 43–57. The University of Arizona Press.
- Guan, P., Zhou, L.-Y., and Li, J. (2012). Trailing (L5) Neptune Trojans: 2004 KV18 and 2008 LC18. *Research in Astronomy and Astrophysics*, 12:1549–1562, 1205.2206.
- Horner, J. and Lykawka, P. S. (2010). 2001 QR322: a dynamically unstable Neptune Trojan? *Monthly Notices of the Royal Astronomical Society*, 405:49–56, 1002.4699.



- Horner, J. and Lykawka, P. S. (2012). 2004 KV<sub>18</sub>: a visitor from the scattered disc to the Neptune Trojan population. *Monthly Notices of the Royal Astronomical Society*, 426:159–166.
- Horner, J., Lykawka, P. S., Bannister, M. T., and Francis, P. (2012). 2008 LC18: a potentially unstable Neptune Trojan. *Monthly Notices of the Royal Astronomical Society*, 422:2145–2151, 1202.3279.
- Horner, J. and Wyn Evans, N. (2006). The capture of Centaurs as Trojans. *Monthly Notices of the Royal Astronomical Society*, 367:L20–L23, arXiv:astro-ph/0511791.
- Kaib, N. A., Roškar, R., and Quinn, T. (2011). Sedna and the Oort Cloud around a migrating Sun. *Icarus*, 215:491–507, 1108.1570.
- Karlsson, O. (2004). Transitional and temporary objects in the Jupiter Trojan area. *Astronomy and Astrophysics*, 413:1153–1161.
- Levison, H. F. and Duncan, M. J. (1994). The long-term dynamical behavior of short-period comets. *Icarus*, 108:18–36.
- Levison, H. F. and Duncan, M. J. (1997). From the Kuiper Belt to Jupiter-Family Comets: The Spatial Distribution of Ecliptic Comets. *Icarus*, 127:13–32.
- Levison, H. F., Shoemaker, E. M., and Shoemaker, C. S. (1997). Dynamical evolution of Jupiter’s Trojan asteroids. *Nature*, 385:42–44.
- Lykawka, P. S. and Mukai, T. (2007). Resonance sticking in the scattered disk. *Icarus*, 192:238–247, 0707.4301.
- Mikkola, S., Brassier, R., Wiegert, P., and Innanen, K. (2004). Asteroid 2002 VE68, a quasi-satellite of Venus. *Monthly Notices of the Royal Astronomical Society*, 351:L63–L65.

- Mikkola, S., Innanen, K., Wiegert, P., Connors, M., and Brassier, R. (2006). Stability limits for the quasi-satellite orbit. *Monthly Notices of the Royal Astronomical Society*, 369:15–24.
- Morais, M. H. M. and Morbidelli, A. (2002). The Population of Near-Earth Asteroids in Coorbital Motion with the Earth. *Icarus*, 160:1–9.
- Morais, M. H. M. and Morbidelli, A. (2006). The population of Near Earth Asteroids in coorbital motion with Venus. *Icarus*, 185:29–38.
- Namouni, F. (1999). Secular Interactions of Coorbiting Objects. *Icarus*, 137:293–314.
- Namouni, F., Christou, A. A., and Murray, C. D. (1999). Coorbital Dynamics at Large Eccentricity and Inclination. *Physical Review Letters*, 83:2506–2509.
- Nesvorný, D. and Dones, L. (2002). How Long-Lived Are the Hypothetical Trojan Populations of Saturn, Uranus, and Neptune? *Icarus*, 160:271–288.
- Parker, A. H., Buie, M. W., Osip, D. J., Gwyn, S. D. J., Holman, M. J., Borncamp, D. M., Spencer, J. R., Benecchi, S. D., Binzel, R. P., DeMeo, F. E., Fabbro, S., Fuentes, C. I., Gay, P. L., Kavelaars, J. J., McLeod, B. A., Petit, J.-M., Sheppard, S. S., Stern, S. A., Tholen, D. J., Trilling, D. E., Ragozzine, D. A., Wasserman, L. H., and Ice Hunters, t. (2013). 2011 HM<sub>102</sub>: Discovery of a High-inclination L5 Neptune Trojan in the Search for a Post-Pluto New Horizons Target. *Astronomical Journal*, 145:96.
- Petit, J.-M., Kavelaars, J. J., Gladman, B. J., Jones, R. L., Parker, J. W., Van Laerhoven, C., Nicholson, P., Mars, G., Rousselot, P., Mousis, O., Marsden, B., Bieryla, A., Taylor, M., Ashby, M. L. N., Benavidez, P., Campo Bagatin, A., and Bernabeu, G. (2011). The Canada-France Ecliptic Plane Survey - Full Data Release: The Orbital Structure of the Kuiper Belt. *Astronomical Journal*, 142:131, 1108.4836.
- Scholl, H., Marzari, F., and Tricarico, P. (2005). Dynamics of Mars Trojans. *Icarus*, 175:397–408.

- Shankman, C., Gladman, B. J., Kaib, N., Kavelaars, J. J., and Petit, J. M. (2013). A Possible Divot in the Size Distribution of the Kuiper Belt’s Scattering Objects. *Astrophysical Journal Letters*, 764:L2, 1210.4827.
- Sheppard, S. S. and Trujillo, C. A. (2006). A Thick Cloud of Neptune Trojans and Their Colors. *Science*, 313:511–514.
- Sheppard, S. S. and Trujillo, C. A. (2010a). Detection of a Trailing (L5) Neptune Trojan. *Science*, 329:1304–.
- Sheppard, S. S. and Trujillo, C. A. (2010b). The Size Distribution of the Neptune Trojans and the Missing Intermediate-sized Planetesimals. *Astrophysical Journal Letters*, 723:L233–L237, 1009.5990.
- Tiscareno, M. S. and Malhotra, R. (2003). The Dynamics of Known Centaurs. *Astronomical Journal*, 126:3122–3131, arXiv:astro-ph/0211076.
- Volk, K. and Malhotra, R. (2008). The Scattered Disk as the Source of the Jupiter Family Comets. *Astrophysical Journal*, 687:714–725, 0802.3913.
- Wiegert, P. A., Innanen, K. A., and Mikkola, S. (1998). The Orbital Evolution of Near-Earth Asteroid 3753. *Astronomical Journal*, 115:2604–2613.

### **Acknowledgements**

We thank Nathan Kaib for making the scattering object model available to us.

We thank Samantha Lawler, Cory Shankman and Nathan Kaib for proof-reading and constructive comments.

M. Alexandersen and B. Gladman were supported by the National Sciences and Engineering Research Council of Canada.

This work is based on observations obtained at the Canada-France-Hawaii Telescope (CFHT). CFHT is operated by the National Research Council of Canada, the Institut

National des Sciences de l'Univers of the Centre National de la Recherche Scientifique of France, and the University of Hawaii.

## **Appendices**

Supporting additional text

Figs. A1, A2, A3, A4

References (20-43)

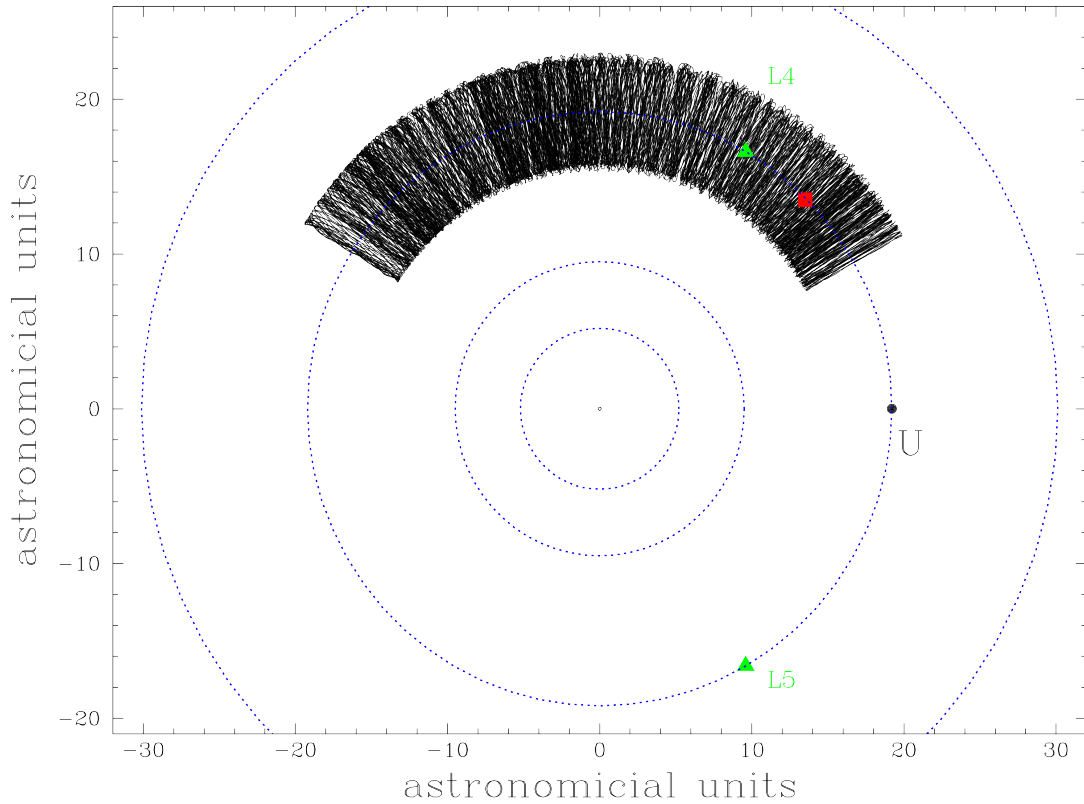


**Fig. 1.** The motion of 2011 QF<sub>99</sub> from its current position (red dot) to 70 kyr, multiple libration periods, into the future. The co-ordinate frame co-rotates with Uranus (on right) and circles show the average orbital distances of Jupiter, Saturn, Uranus and Neptune. Green triangles denote the L4 (upper) and L5 (lower) Lagrange points. The visible rapid radial oscillation occur on the time scale of one heliocentric orbit, while the angular extent around the Sun is the slower libration around the L4 Lagrange point.

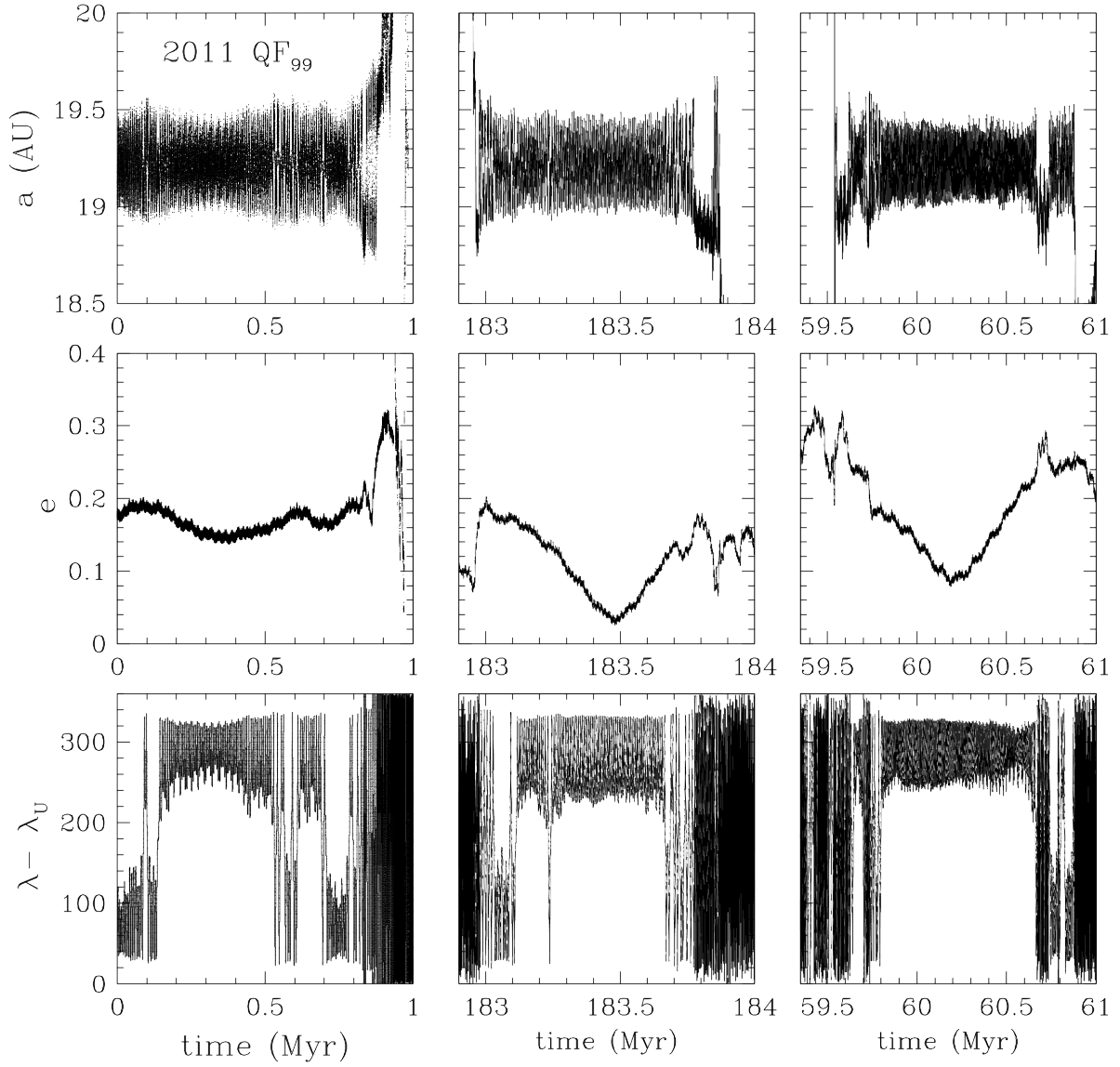


**Fig. 2.** Left column: Evolution of the semi-major axis  $a$ , eccentricity  $e$  and resonant angle  $\lambda - \lambda_U$  of 2011 QF<sub>99</sub> for 1 Myr into the future. Centre and right columns: Evolution for two temporary Uranian co-orbitals from our dynamical simulations for intervals in which their evolution is similar to that of 2011 QF<sub>99</sub>, showing that Centaurs can naturally become temporarily trapped Uranian Trojans. Times are from the initial condition for the  $a_0 > 34$  AU scattering orbit.

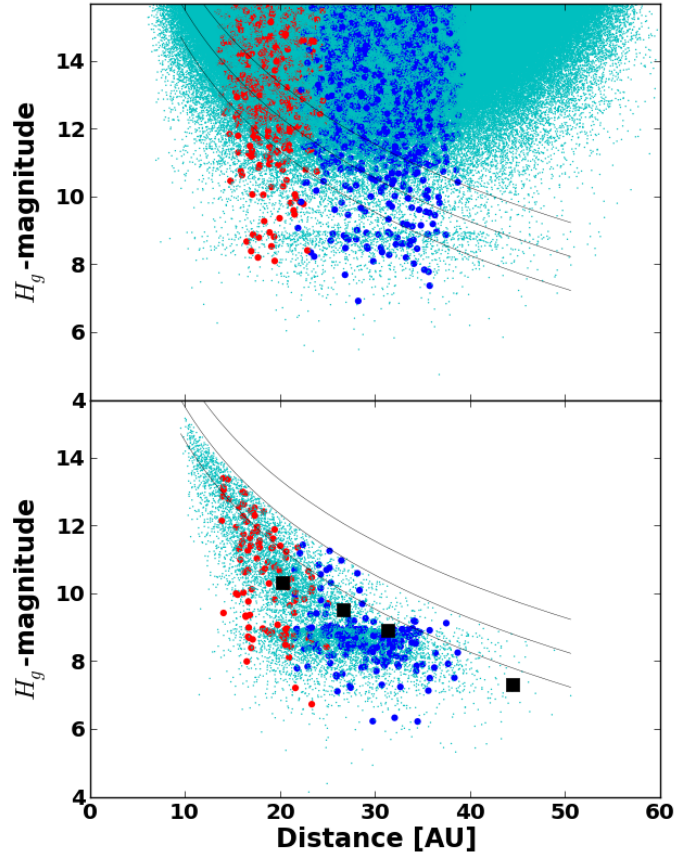


**Fig. 3.** Top: The intrinsic model population of Centaurs/scattering objects (tiny cyan dots), Uranian co-orbitals (red) and Neptunian co-orbitals (blue). The three populations are plotted with the relative fractions from the model, but the co-orbitals have larger symbols to make them more visible. Bottom: The objects detected by our survey simulator, using the same colour scheme. The large black squares are the four real  $a < 34$  AU detections from our calibrated work, 2011 QF<sub>99</sub> being the upper-left one. In both plots, the black curves correspond to apparent magnitudes  $m_g = 24.25, 25.25$  and  $26.25$ , from bottom to top, which are roughly the survey limits of CFEPS (Petit et al., 2011), our new observations and a deep survey for Neptunian Trojans (Sheppard and Trujillo, 2010b), respectively. The effect of the divot  $H$ -mag distribution can easily be seen around  $H_g = 9.0$ , allowing the simulated detections to not be dominated by  $H_g > 11.0$  objects.

# Appendices

## Known Co-orbitals of other planets

There are objects known to be in co-orbital motion with several of the planets in the Solar System, both as long-term stable, presumably primordial (by which we mean  $\sim 4$  Gyr lifetimes) populations and also as temporary captures. Working outwards from the Sun:

**Venus** has a temporary quasi-satellite, which was the first known quasi-satellite of a major planet (Mikkola et al., 2004).

**Earth** has an unstable horseshoe companion, 3753 Cruithne (Wiegert et al., 1998), while 2002 AA<sub>29</sub> (Connors et al., 2002) exhibits both temporary horseshoe and quasi-satellite behaviours. 2003 YN<sub>107</sub> (Connors et al., 2004) is currently a quasi-satellite while 2010 TK<sub>7</sub> is a temporary L4 Trojan.

**Mars** has four known Trojans, all of which are believed to be stable on Gyr time scales (Scholl et al., 2005).

**Jupiter** has more than 3000 known long-term stable Trojan asteroids in its Trojan clouds, which are believed to outnumber the main asteroid belt (Levison et al., 1997). In terms of temporary co-orbitals, only a few very short-term,  $< 1$  kyr, captures have been identified (Karlsson, 2004).

**Saturn** does not have any known co-orbitals, and its co-orbital phase-space is believed to be highly unstable (Nesvorný and Dones, 2002). Orbital simulations (Horner and Wyn Evans, 2006) show temporary captures are possible.

**Uranus** has one known temporary ( $\sim 20$  kyr) horseshoe companion (de la Fuente Marcos and de la Fuente Marcos, 2013) and 2011 QF<sub>99</sub>, the temporary L4 Trojan reported here. The Uranian co-orbital region is thought to be mostly unstable (Nesvorný and Dones, 2002) although some stable niches may exist (Dvorak et al., 2010).

**Neptune** was recently discovered to have a large stable Trojan population which might outnumber the Jovian Trojans (Chiang and Lithwick, 2005). Neptune currently has nine known Trojans, of which 6 are known to be stable over the age of the Solar System (Shep-



pard and Trujillo, 2006, 2010a; Parker et al., 2013). The first discovered Neptunian Trojan, 2001 QR<sub>322</sub> (Chiang et al., 2003), as well as 2008 LC<sub>18</sub>, have orbital uncertainties straddling the boundary between long-term stable and temporary librators and may be short-lived (Brasser et al., 2004; Horner and Lykawka, 2010; Horner et al., 2012; Guan et al., 2012) although primordial orbits are also possible. The Canada-France-Ecliptic-Plane-Survey (CFEPS) discovered the first Neptunian Trojan (2004 KV<sub>18</sub>, Fig. A2 left column) which is beyond doubt unstable on a short time scale (Petit et al., 2011; Gladman et al., 2012; Horner and Lykawka, 2012). Recently, others (de la Fuente Marcos and de la Fuente Marcos, 2012a,b) have run short numerical integrations of known Centaurs and identified a temporary Neptunian quasi-satellite, three temporary Neptunian Trojans and a temporary Neptunian horseshoe, although some of these classifications are still insecure. Maybe surprisingly, the number of known transient Neptunian co-orbitals are now of order the same as the long-term stable co-orbitals.

## Our recent study

Our study used CFHT to cover a 20 sq.deg. patch of sky on the ecliptic near RA=2 hr, Dec=15°, in the  $r$ -band filter. This direction was selected to optimise the search for resonant objects, as RA=2 hr is  $\approx 60^\circ$  ahead of Neptune, the region in which L4 Trojans reside, as well as where n:2 and n:3 resonant object come to pericentre (Gladman et al., 2012). The searched fields were also near the Uranian L4 point (Fig. 1). Discovery observations were obtained in October 2011 and tracking observations were made throughout 2011 and 2012, succeeding in a 100% tracking fraction for  $m_r < 24.55$ . The detection efficiency was measured by implanting fake objects into the observations. The search had a detection efficiency of 88% for objects brighter than  $m_r = 23.0$  with a magnitude limit at  $m_r = 24.55$ . Here, the magnitude limit is quoted as the magnitude at which the detection efficiency has dropped to half of the maximum efficiency. The observations were searched for objects moving at rates from 0.4"/hr to 10.3"/hr, corresponding to distances between  $\sim 10$  AU

and over 300 AU. Additional detail on the survey is not relevant to this paper and will be described in a future publication.

### **Details on classification of 2011 QF<sub>99</sub>**

After a short integration, which showed that 2011 QF<sub>99</sub> was librating around the Uranian L4 point, we ran a 10 Myr classification using the Solar System Beyond Neptune classification algorithm (Gladman et al., 2008). In that algorithm, instead of using a Gaussian covariance matrix based on the rms scatter of the observations, a Monte-Carlo technique searches out from the best-fit (minimum residual) orbit for the ‘maximal’ and ‘minimal’ semi-major axis orbits which are judged acceptable given the residual pattern of the best fit. In this case the three semi-major axes are 19.167 AU, 19.175 AU, and 19.183 AU (these are not Gaussian errors, but should rather be interpreted as the maximum allowable range). These three orbits are then integrated for 10 Myr into the future to look for resonant behavior. For 2011 QF<sub>99</sub>, all 3 orbits escape the co-orbital 1:1 resonance in less than 3 Myr, so 2011 QF<sub>99</sub> is not classified by this algorithm as a stable resonant object; instead it is only temporarily (by astronomical standards) in the co-orbital state. Fig. A1 shows the three evolutions for the next 1 Myr into the future. As shown (and also true in all other experiments we have conducted with different time steps), 2011 QF<sub>99</sub> always executes 10 or more angular librations of the  $\phi_{11}$  resonant argument around the L4 point, over the next 70 kyr or more. Due to the chaotic nature of the resonance dynamics, by this point the orbits have sufficiently separated that they show different evolutions as to when they exit the L4 libration. This exit is usually into another form of co-orbital behaviour (transition to an L5 libration or a horseshoe orbit). As is usual for such a chaotic trajectory, there is a range of times to exit the resonance; we find that the co-orbital status of 2011 QF<sub>99</sub> is very likely to be maintained for the next half million years. On time scales of a few Myr all orbits we have integrated (even those not formally consistent with the astrometry; see main text) leave the resonance to rejoin the Centaur population from which the object must have come.

## Details on dynamical integrations

The **dynamical integrations** computed to model the steady-state distribution of scattering objects in the  $a < 34$  AU region for this work were set up using a subset of particles from the Kaib et al. (2011 - KRQ11 henceforth) (Kaib et al., 2011) TNO population model. This subset consisted of 17,800 particles with initial semi-major axis  $34 \text{ AU} < a < 200 \text{ AU}$  and which had their semi-major axes deviate by more than 1.5 AU during the last 10 Myr of the KRQ11 model integrations. This populations of scattering TNOs were used as the initial conditions for the orbital integrations in this work. Two different KRQ11 models were used independently: one generated from a primordial inclination distribution that was already dynamically hot when the particles left the giant planet region 4 Gyr earlier (the “hot” model), the other using an initially cold distribution (the “cold” model) (Kaib et al., 2011; Shankman et al., 2013).

To perform this computation, we used the N-body code SWIFT-RMVS4 (provided by Hal Levison, based on the original SWIFT (Levison and Duncan, 1994)). A base time step of 73 days was used and the orbital elements was output every 300 years for any particle which at that moment had  $a < 34$  AU. The gravitational influences of the four giant planets were included. Particles were tracked until they hit a planet, reached a minimum heliocentric distance  $r_{min} < 6$  AU, reached a maximum heliocentric distance  $r_{max} > 2000$  AU or the final integration time of 1 Gyr was reached.

The goal of these orbital integrations was twofold: to search for temporary co-orbital trapping and to construct the steady-state orbital distribution of scattering TNOs which reach the giant planet region, chosen to be the  $a < 34$  AU region. The steady-state orbital distribution is expressed as a grid with  $a < 34$  AU,  $e < 1.0$ ,  $i < 180^\circ$ , with cells of volume  $0.5 \text{ AU} \times 0.02 \times 2^\circ$ . The cumulative time spent by all particles in each cell is normalized to the total time spent by all particles in all cells in the  $a < 34$  AU region. This illustrates the steady-state distribution of objects in the  $a < 34$  AU region (see Fig. A3) supplied by the scattering TNO population. This “residence time” probability distribution (Bottke et al.,

2000) can be interpreted as the steady-state fraction of scattering TNOs in each cell. Fig. A3 shows two projections of the residence time probability distributions of the  $a < 34$  AU region for the two KRQ11 population models. From these plots it is clear the scattering TNO population enters the giant planet region ( $a < 34$  AU) at moderate eccentricities and inclinations. Although the hot model does produce higher inclinations, it is clear from Fig. A3, and is confirmed by our survey simulator, that the choice of input model does not make a large difference for our results. We therefore only describe results from the simulations using the KRQ11 “hot” model.

This is not the first work of its kind to perform numerical integrations in order to construct the steady-state population of Centaurs with  $a < 34$  AU from a scattering TNO population. Some works present numerical integrations of Centaurs (both known and test populations) (Tiscareno and Malhotra, 2003; Dones et al., 1999; Horner and Wyn Evans, 2006) initially within the giant planet region. Those that have modelled the evolution of scattering TNOs from the Scattered Disk into the  $a < 34$  AU Centaur region (Levison and Duncan, 1997; Volk and Malhotra, 2008) did not search for temporary (often  $< 100$  kyr) co-orbital captures.

Work similar to that presented here has been performed simulating near Earth asteroids captured as temporary co-orbitals of Earth (Morais and Morbidelli, 2002). They found that the Earth’s temporary co-orbitals often experience several co-orbital phases, each of average duration 25 kyr (none longer than 1 Myr).

**To diagnose whether particles are co-orbital**, the orbital history (at 300 year output intervals) was scanned using a running window 30 kyr long. This window-size was chosen, as this is several times longer than the typical Trojan libration period. While the formal definition of co-orbital is that the resonant angle  $\phi_{11} = \lambda - \lambda_{Planet}$  librates, detecting this is difficult to automate. As an automatic process is necessary to filter the large amounts of output from our dynamical simulations (110 Gb), we used a simpler algorithm which we believe diagnoses co-orbitals well. A particle was classified as a co-

orbital if, within the running window, both its average semi-major axis was less than 0.2 AU from the average semi-major axis of a given planet and no individual semi-major axis value deviated more than 0.65 AU from that of the planet. If these criteria were met, the orbital elements and current integration time for that particle (at the time-centre of the window) were output to indicate co-orbital motion in that window. The window centre then advances by a single 300-year output interval and performs the diagnosis determination again. In this manner, consecutive identifications of a particle in co-orbital motion with a planet can be recorded as a single “trap” until the object is scattered away. A minor shortcoming of this method of co-orbital identification is that the beginning and end of each trap is not diagnosed well due to the ends of the window not falling entirely within the trap at these times. This method provides us with an estimate of the length of a given trap, each of which must be greater than 30 kyr to be diagnosed by this analysis.

Numerical integrations of known Centaurs have previously been performed (Horner and Wyn Evans, 2006) in order to study the capture of Centaurs as temporary co-orbitals of the giant planets. That study found that captures are generally short (10-100 kyr, none greater than 500 kyr) with 0.29% of 23 328 Centaur clones experiencing a co-orbital capture during a 3 Myr simulation, of which 15%, 80%, 5% and 0% of these captures at Jupiter, Saturn, Uranus and Neptune, respectively. The previous study used clones of the known Centaurs for initial conditions, a starting condition heavily biased towards smaller semi-major axes.

In the work presented here, where Centaurs are provided from a bias-free external scattering disk, we find that the average length of captures in co-orbital motion with Uranus is 114 kyr and with Neptune is 84 kyr. We were surprised to find that objects that experience at least one episode of co-orbital capture have a median of 2 captures with Uranus or 4 captures with Neptune. Objects typically escape with low relative velocities, so multiple temporary captures is not surprising. Some objects experience temporary co-orbital captures with both planets (see Fig. A2, right column). Due to the  $r_{min} = 6$  AU distance cut in the integrations, which may remove Saturn crossing Centaurs before they

get their full chance to get trapped, we did not reliably measure the Saturnian trapping fraction, but estimate it at  $\ll 0.1\%$  of the incoming scattering population.

**Resonant island classification.** For each time step a particle has been deemed co-orbital, we then determine in which of the four resonant islands the particle is librating, i.e. whether it is a horseshoe, L4 Trojan, L5 Trojan, or quasi-satellite. As for the co-orbital detection earlier, this is also hard to automate, especially because complex variations and combinations can exist for high inclinations. For our classification algorithm, we examine the behavior of the resonant angle ( $\phi_{11} = \lambda - \lambda_p$ ) in each 30 kyr window. If the object remained in the leading or trailing hemisphere during a window, we assigned the particle to the L4 or L5 state (respectively). If it changed hemispheres near  $\phi_{11} = 180^\circ$  at any time during the interval, then it was labelled a horseshoe orbit. The remainder is assumed to be quasi-satellites, as they must all be co-orbitals that cross between hemispheres at  $\phi_{11} = 0^\circ$  and not at  $180^\circ$ .

## Quasi-satellites

Quasi-satellites make up 7% of the steady-state Uranian co-orbitals and 13% of the steady-state Neptunian co-orbitals in our numerical integrations. This is thus a rare state, but of great dynamical interest (Namouni, 1999; Namouni et al., 1999; Connors et al., 2002; Mikkola et al., 2004; Connors et al., 2004; Mikkola et al., 2006; de la Fuente Marcos and de la Fuente Marcos, 2012a). There is currently one known temporary quasi-satellite of Neptune (de la Fuente Marcos and de la Fuente Marcos, 2012a). The current existence of one known temporary quasi-satellite, out of a total of  $\sim 6$  known temporary Uranian and Neptunian co-orbitals, fits into our general picture of temporary traps in co-orbital states. Fig. A4 depicts the semi-major axis, eccentricity, and resonant angle evolution of two temporary quasi-satellite captures found in our numerical integrations. The capture shown on the left is a quasi-satellite with Neptune for a duration of 694.5 kyr before it scatters away. The capture on the right in Fig. A4 remains a quasi-satellite with Uranus for 1.45 Myr before leaving the co-orbital state.

## Survey Simulator

The CFEPS Survey Simulator works by either drawing random objects from a ready-made list of objects or from a model orbital distribution within the simulator. The object is then allocated an  $H$ -magnitude, drawn from a model  $H$ -mag distribution. The simulator then proceeds to test whether or not a given object would be detectable by any of the surveys that it has been set up to simulate, taking into account the position of the observed fields, the position of the object, the detection efficiency as a function of object magnitude, as well as rate and direction of motion of the object. We only use our current campaign and CFEPS, as those are the only observations for which we have access to all the required information needed to simulate the survey. For this paper, we draw scattering objects with  $a < 34$  AU from the output of the dynamical simulation. However, the dynamical simulation only generated a few hundred co-orbital objects and their distribution was therefore insufficiently sampled to be used directly as a source for the survey simulator. Instead we drew co-orbitals from a model distribution set up to resemble the co-orbital distribution found in the dynamical simulation, with relative fractions in each population (Centaur, Uranian Trojans, Neptunian horseshoes, etc.) set to be the same as that found from the dynamical simulation.

### $H$ -mag distribution

Minor body populations can typically be well represented, over some range of magnitudes, by an exponential absolute magnitude,  $H$ , distribution of the form

$$\frac{dN}{dH} \propto 10^{\alpha H}$$

where  $dN/dH$  is the number of objects per  $H$ -mag. The cumulative  $H$ -mag distribution can be described by integrating this to get

$$N(< H) \propto 10^{\alpha H}$$

where  $N(< H)$  is the cumulative number of objects brighter than  $H$ . Note that both distributions have the same exponent.

As described in the main text, a single exponential  $H$ -mag distribution does not agree with our observations; the single exponential distribution predicts that small ( $H_g > 11.0$ ) objects should completely dominate, accounting for 81% of the simulated detections, whereas our observations have no such objects. The probability of 0 small objects out of 4 detections given this expectation is 0.12%, rejecting the single exponential distribution at  $> 99\%$  confidence. Previous work (Shankman et al., 2013) has shown that the scattering disk objects cannot follow a single exponential function and is better modelled by a divot distribution. The divot  $H$ -mag distribution is simply two different distributions of the form above, one relevant for magnitudes brighter than the divot, the other relevant for magnitudes fainter than the divot, with a discontinuity at the divot. As we are pursuing the notion that the temporary co-orbitals are temporarily captured Centaurs, which themselves are scattered disk objects scattered inwards, it is to be expected that the temporary co-orbitals and Centaurs follow the same  $H$ -mag distribution as the scattering disk. Adopting the divot  $H$ -mag distribution produces results in better agreement with our observations (see Fig. 3); small ( $H_g > 11.0$ ) objects now only provide 23% of the detections. The probability of detecting 0 small objects out of four given this expectation is 36%, so this distribution is not in conflict with the observations and we adopt it. As the values of the contrast and post-divot slope are not uniquely determined (Shankman et al., 2013), we explored reasonable ranges but found less than factor of two changes in the detected fraction of co-orbitals.

To further illustrate the improvement in using a divot  $H$ -mag distribution over the single exponential distribution, we test our four detections against the simulated detections using the Kolmogorov-Smirnov (KS) and Anderson-Darling (AD) tests. Using a single exponential  $H$ -mag distribution, the KS test gives 0.01% and 0.15% probability that our four detections were drawn from the same  $H$ -mag and distance distributions as the simulated



detections, respectively. The AD test gave 0.04% and 0.03% for those same parameters. Using the divot  $H$ -mag distribution, the KS test gives 68% and 28% probability that our four detections were drawn from the same  $H$ -mag and distance distributions as the simulated detections (see Fig. 3), respectively. The AD test gave 66% and 7.3% for those same parameters. Thus the single exponential is rejectable at greater than 99% confidence for all four tests, while the divot distribution is not rejectable at 95% confidence by any of the tests.

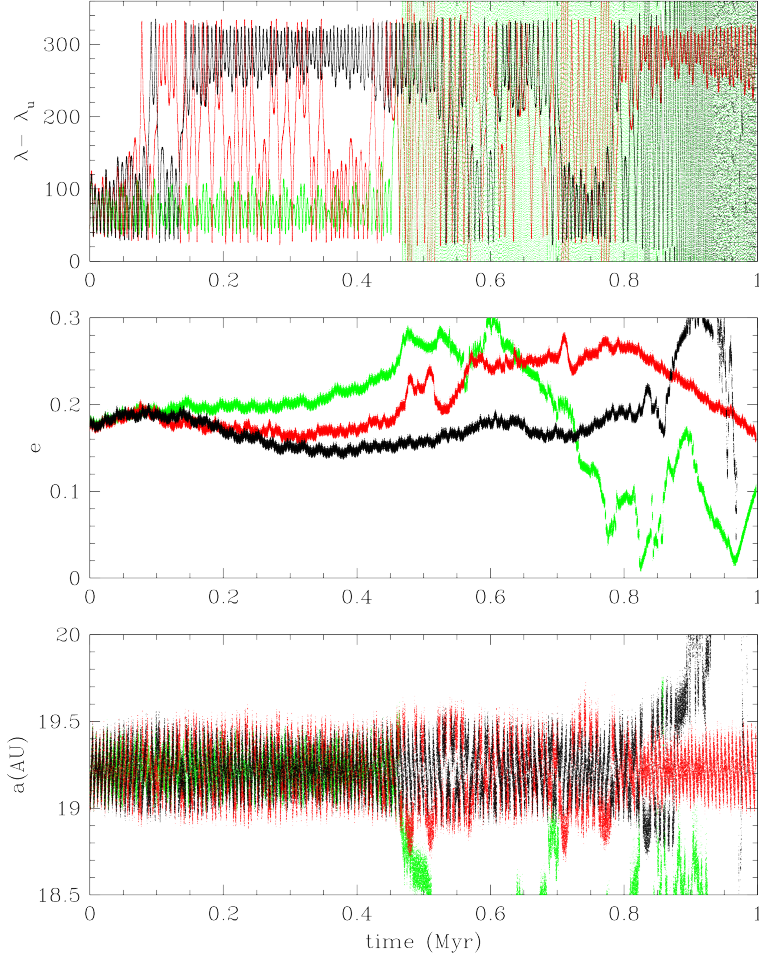


**Fig. A1.** The future evolution of 2011 QF<sub>99</sub>, from a numerical integration of the best-fit orbit (black) as well as the smallest and largest semi-major axis orbits within the uncertainty (green and red, respectively). Notice that all three clones remain as L4 Trojans for at least 70 kyr and remain co-orbital for at least 450 kyr. The nominal orbit (black) switches back and forth from L4 to L5, before a horseshoe period at  $t \approx +800$  kyr and then escape from the resonance at  $t \approx +880$  kyr. The small- $a$  clone (green) remains around L4 the longest, until breaking loose around  $t \approx +450$  kyr and never getting recaptured. The large- $a$  clone (red) is the most stable and remains in or near the co-orbital state for the entire 1 Myr shown here, before leaving soon after. The detailed evolution is highly chaotic, but all orbits are L4 Trojans in the near future and remain co-orbital on  $\sim 400$  kyr time scales.

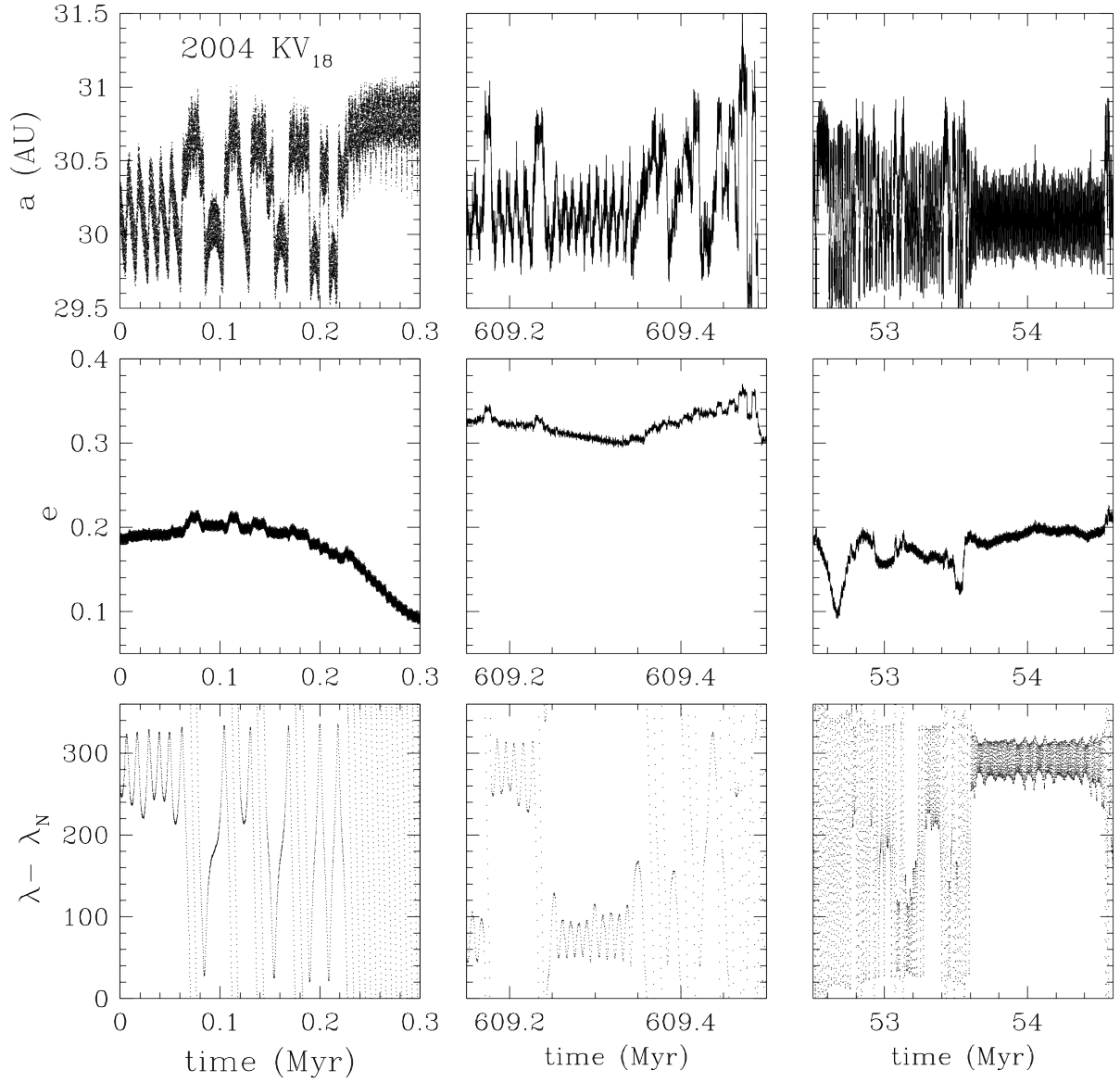


**Fig. A2.** Left column: Evolution (for 0.3 Myr into the future) of the semi-major axis  $a$ , eccentricity  $e$  and resonant angle  $\lambda - \lambda_N$  of 2004 KV<sub>18</sub> (the certainly-unstable Neptunian Trojan (Gladman et al., 2012; Horner and Lykawka, 2012)). Centre and right columns: Evolution for two temporary Neptunian co-orbitals from our dynamical simulations for intervals in which their evolution is similar to that of 2004 KV<sub>18</sub>. Note: The object on the right is the same object as in right column of Fig. 2. This object experiences co-orbital motion with both Uranus and Neptune, with  $\sim 5$  Myr between the two temporary captures.

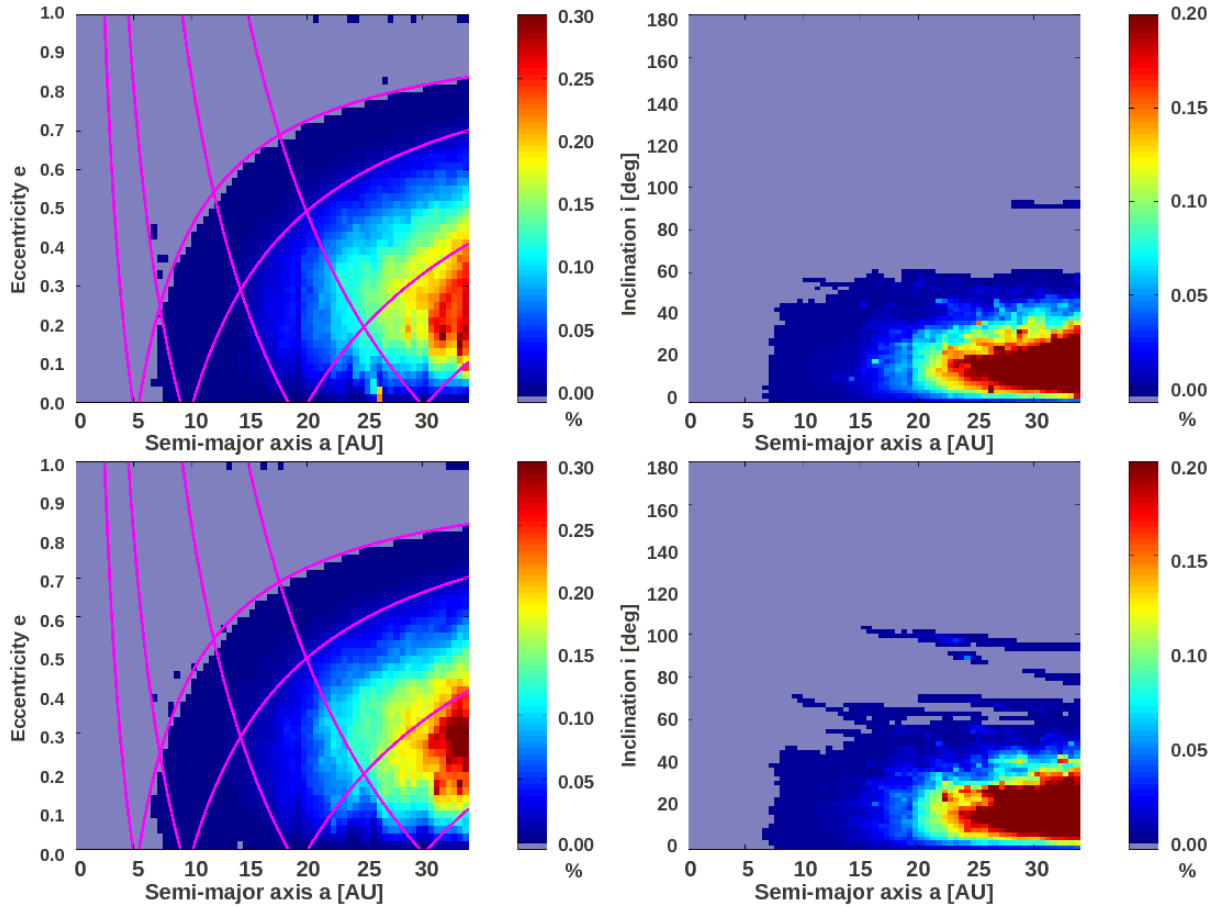


**Fig. A3.** Residence time probability distributions, from the initially cold (top) and hot (bottom) KRQ11 model; the two different initial populations clearly produce very similar  $a < 34$  AU steady-states. To monitor the orbital evolution of each particle, a grid of  $a$ ,  $e$ ,  $i$  cells was placed throughout the giant planet region from  $a < 34$  AU,  $e < 1.0$ , and  $i < 180^\circ$  with volume  $0.5 \text{ AU} \times 0.02 \times 2^\circ$ . The  $a$ ,  $e$  plot is summed over  $i$ , and the  $a$ ,  $i$  plot is summed over  $e$ . The color scheme represents the percentage of the steady-state Centaur population contained in each bin; Red colors represent cells where there is a high probability of particles spending their time. The curves indicate Jupiter, Saturn, Uranus, and Neptune crossing orbits.

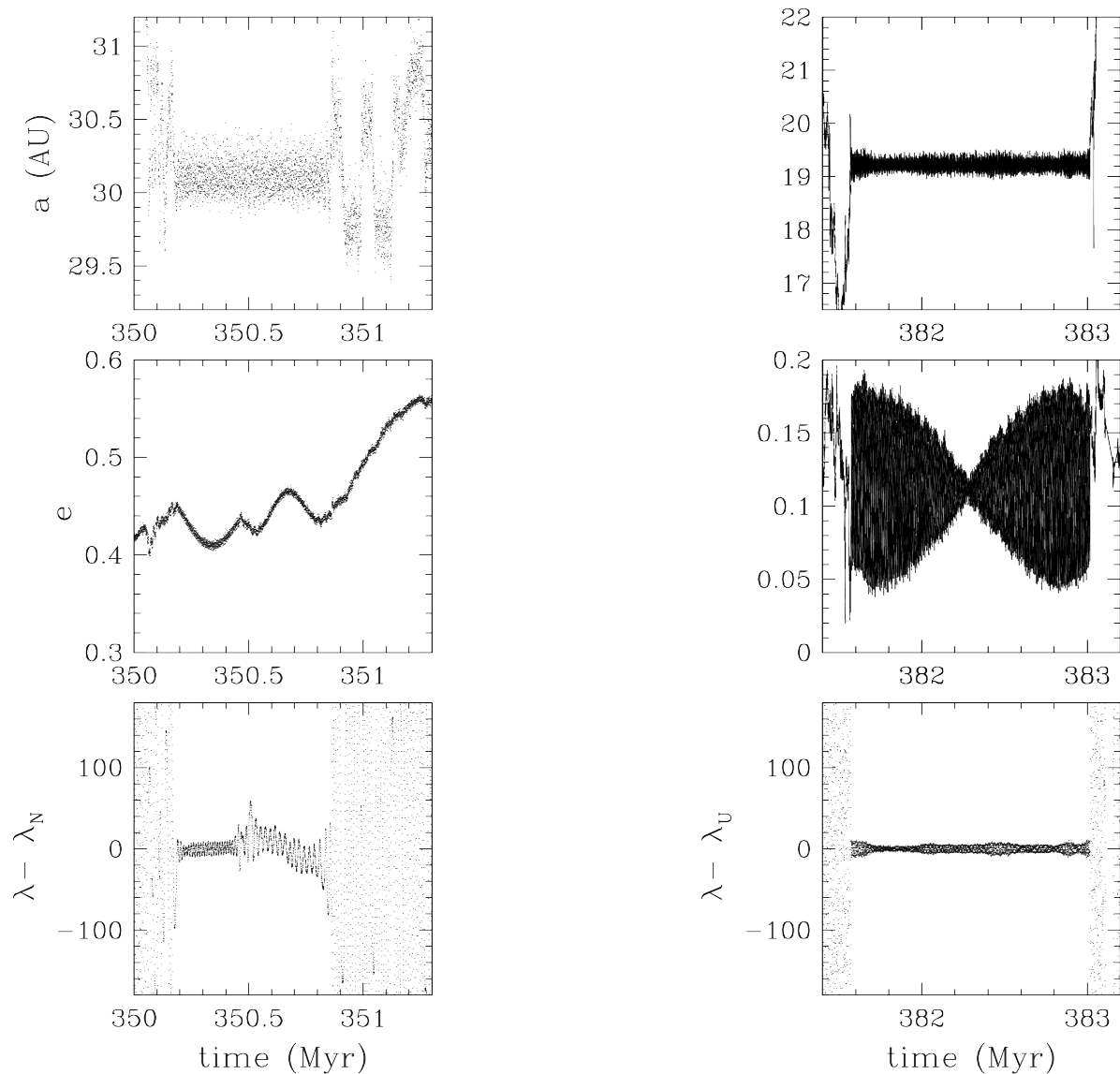


**Fig. A4.** Evolution of the semi-major axis  $a$ , eccentricity  $e$  and resonant angle  $\lambda - \lambda_{Planet}$  for two temporary quasi-satellites captures from our dynamical simulation, one Uranian (right) and one Neptunian (left). Note the different scales.